Improving Power Efficiency of AESA System with GaN Supply-Modulated Power Amplifier

Pham Cao Dai(✉), Le Dai Phong, Luu Van Tuan, and Nguyen Hoang Nguyen

Institute of System Integration, Le Quy Don Technical University, 236 Hoang Quoc Viet, Hanoi, Vietnam
daipc.isi@lqdtu.edu.vn

Abstract. This paper presents an analysis of using GaN supply-modulated (SM) power amplifier (PA) in an active electronically scanned array (AESA) system to improve system power efficiency. Specifically, the paper details a 4-W X-band GaN SM PA with power-added efficiency (PAE) of above 50% at 9.4 GHz frequency. The proposed PA achieves the PAE of above 35% over 800 MHz bandwidth and 40% in 10 dB output power back-off range. The simulation results show that the system PAE increases about 14–18% at the same condition of the array amplitude distribution and array scales by using GaN SM PA.

Keywords: Active electronically scanned array · GaN · Supply-modulated power amplifier · Power distribution · Operation range

1 Introduction

Recently, the active electronically scanned array (AESA) system [1–3] is widely researched, developed, and applied in radar and multi-function wireless systems. An AESA system uses solid-state devices and consists of an active phased array antenna where each of its elements is connected to a transceiver. This design can bring about high reliability, a wide dynamic range, high sensitivity, anti-electromagnetic interference, flexibility, and versatility, etc. [2, 4] whereas conventional models cannot because they utilize only one transceiver for all the antenna elements. For instance, the beamforming technique in an AESA system allows to synthesis transmitting/receiving pattern flexibly, scan the antenna spatially, and establish the multichannel for communication, detection, or tracking of different targets simultaneously.

However, there exist some disadvantages in an AESA system. The systematic design of AESA is incredibly complicated to achieve a wide scanning range, and avoid grating lobes, the distance between modules usually ranges from half-wavelength to wavelength [5]. It's only about 1.6 to 3.2 cm at 9.4 GHz. This makes the placement of the transceiver modules and system cooling more difficult.

Furthermore, the process of synthesizing the desired antenna pattern and reducing the side-lobe level usually leads to an unequal power distribution over the antenna aperture. This differs the output power of transmitter modules, which is the unwanted effect.

N.-S. Vo et al. (Eds.): INISCOM 2021, LNICST 379, pp. 142–155, 2021.
https://doi.org/10.1007/978-3-030-77424-0_12

Figure 1 illustrates a Taylor-$\overline{n}$ distribution [5] with $n = 3$ and a side-lobe level of -25 dB used in an AESA system with the 16×16-element array.

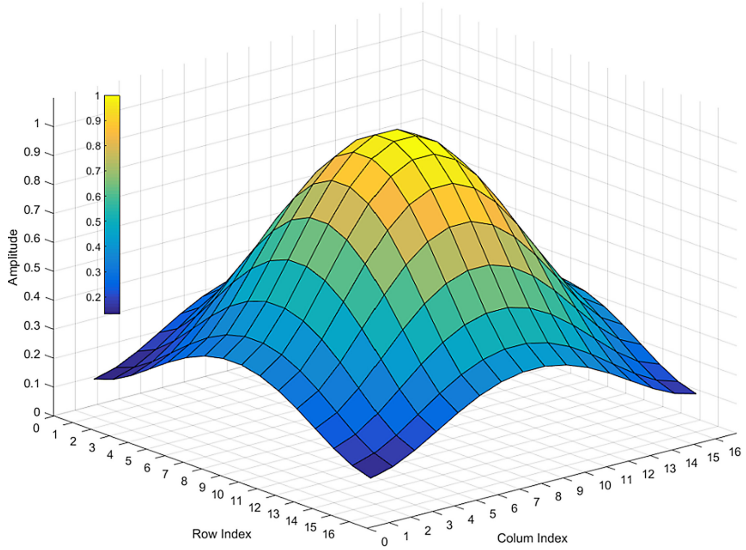

Fig. 1. Taylor $\overline{n}$ distribution with n = 3 and -25 dB side lobe level of a 16×16-elements Array

Due to the limited system space and the varied power distribution, it is necessary to improve the power efficiency and decrease the power consumption of the system, especially to enhance the quality of power amplifier (PA) because they are the largest power-consuming components in the system. In the AESA system, the PA is required to achieve high efficiency and this parameter must be maintained when the PA operates in the wide range of the output power.

The paper analyzes the power efficiency of an AESA system with beamforming, power distribution to result in a low side-lobe level, and changing of transmitting power according to its operating range. In addition, the paper introduces a design of an X-band GaN supply-modulated power amplifier (SM PA) [6, 7] used in an AESA system, which can improve the system power efficiency. The power efficiency of system is evaluated by simulating its operation in different power distributions and diverse array scales.

2 Power Efficiency of AESA System

2.1 Power-Added Efficiency of AESA System

The power efficiency of an AESA system depends on many units of system as PAs, Process unit, Power supply unit, etc. In this paper, we only consider the largest power-consuming components [8] in the AESA system, the PAs.

The power-added efficiency (PAE) of the PAs, given by:

$$PAE(\%) = \frac{P_o - P_i}{P_{DC}} \cdot 100(\%) \tag{1}$$

in which P_o is the output power; P_i is the input power; P_{DC} is the supplied DC power consumption.

Thus, the total PAE of an N-Transceiver AESA system PAE_{AESA} is as follows:

$$PAE_{AESA}(\%) = \frac{\sum_{k=1}^{N}(P_{ok} - P_{ik})}{\sum_{k=1}^{N} P_{DCk}} \cdot 100(\%) \tag{2}$$

where P_{ok}, P_{ik} are the output and input power of the k^{th} PA, respectively, P_{DCk} is the supplied DC power consumption of the k^{th} PA.

By applying Eq. (1), we have:

$$P_{DCk} = \frac{P_{ok} - P_{ik}}{PAE_k} \cdot 100 \tag{3}$$

where PAE_k is the PAE of the k^{th} PA.

Substituting Eq. (3) in Eq. (2), we obtain:

$$PAE_{AESA}(\%) = \frac{\sum_{k=1}^{N}(P_{ok} - P_{ik})}{\sum_{k=1}^{N} \frac{P_{ok} - P_{ik}}{PAE_k}}(\%) \tag{4}$$

Equation (4) shows that the PAE of the system directly depends on the PAE of every PA in the array with the same output power.

2.2 Beamforming and Power Distribution

It is known that an AESA radar is able to gain the desired beam pattern of shape and direction with a reduced side-lobe ratio by controlling amplitude and phase of signals in receiver/transmitter modules using the appropriate coefficients. The formula synthesizing a beam pattern [5] for a linear antenna-element array is below:

$$F(u) = \sum_{n=1}^{N} A_n \cdot exp\left[j2\pi(n-1)u\right] \tag{5}$$

where $F(u)$ is a function of angle θ; A_n is the excitation coefficient of the n^{th} element; N is the length of array; u is a variable given by:

$$u = \frac{d}{\lambda} \cdot (sin\theta - sin\theta_0) \tag{6}$$

in which θ_0 is the desired angle of the beam pattern.

In order to synthesize a specific beam pattern and reduce the side-lobe level, we exploit a certain distribution of excitation coefficients. A 16 × 16-element array using the Taylor $\overline{n}$ distribution with $n = 3$ and -25 dB side-lobe level (see Fig. 1) on both dimensions creates a beam pattern as illustrated in Fig. 2.

The Taylor $\overline{n}$ distribution shows that to achieve the -25 dB side-lobe level of beam pattern, the element of array edge is only 0.1314 in signal amplitude if normalizing signal amplitudes (the magnitude of the center element is 1.0). Thus, the signal power distribution over the array antenna aperture ranges in 17.63 dB.

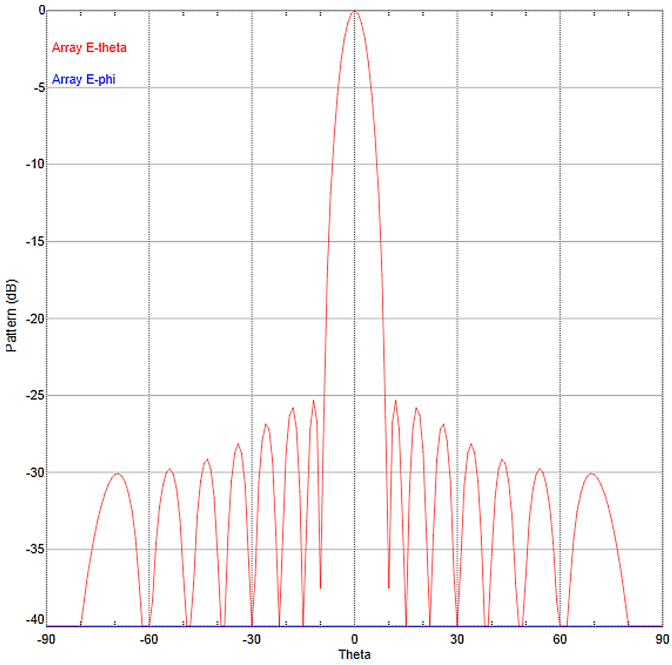

Fig. 2. The beam pattern of 16 × 16-element array antenna using 2D Taylor $\overline{n}$ distribution

In fact, the beamforming is implemented by using either the entire array or its sub-arrays depending pre-defined requirements. These beamforming methods are used in different functions and have different power distributions.

2.3 Operation Range and Transmitting Power

A wireless system does not always operate at its designed maximum distance in a real application to guarantee its functional stability. During operation, the operation range can be changed due to actual requirements. In addition, the changes in encoding, signal bandwidth, data rate etc. lead to change in receiver sensitivity, resulting in change in maximum operation range of system. According to the Friis transmission formula [9], the operation range formula of wireless system is given by:

$$R_{max} = \sqrt{\frac{P_t \cdot G_t \cdot G_r \cdot \lambda^2}{P_{sen} \cdot (4\pi)^2}} \tag{7}$$

where R_{max} is the operation range, P_t is the transmitter power, P_{sen} is the receiver sensitivity, G_t, G_r are the gain of the transmitting and receiving antennas, respectively, and λ is the wavelength.

In a radar system, the transmitter radiates signals out into space. When they meet a target, such signals are reflected and come back to the receiver. Therefore, the operating range formula [10] is given by:

$$R_{max} = \sqrt[4]{\frac{P_t \cdot G_t \cdot G_r \cdot \lambda^2 \cdot \sigma}{P_{sen} \cdot (4\pi)^2 \cdot L_{ges}}} \tag{8}$$

where σ is the target's effective reflection area, and L_{ges} is the loss coefficient.

From Eq. (7) and Eq. (8), the system's operating range is proportional to the square root (fourth root in the radar systems) of the transmitting power. Theoretically, if a system operates at a short distance, its transmitting power can be reduced corresponding to the square root (or fourth root) ratio while the system still works normally.

A current solution for radar systems whose operating ranges change is to properly modify their repetitive frequency, in which the duty of signal is varied but the output peak-power is remained. Thus, PAs always operate at their maximum power levels. However, this is not an optimum solution due to the restriction on controlling parameters of signal pulses and characteristics of the modulation code.

In short, the array antenna elements of an AESA system have inequivalent output power varied with time and position in a wide range during the process synthesizing a beam pattern and changing the operating function/range. Hence, PAs should have high PAEs and maintain them in a broad range of output power to improve the power efficiency for an AESA system. The PAE of a conventional PA achieves the highest value with the maximum output power and decreases rapidly with the decrease of the input power (output power, respectively). From Eq. (7), as a result, the AESA system will not achieve high performance with conventional amplifiers. By exploiting the advantages of GaN technology [11] with the controllable drain bias voltage corresponding to the required output power, the GaN SM PA could satisfy the above requirements. Therefore, it would be appropriate for the AESA system.

3 GaN Supply-Modulated Power Amplifier Design

We propose to use a GaN SM PA whose schematic is shown in Fig. 3.

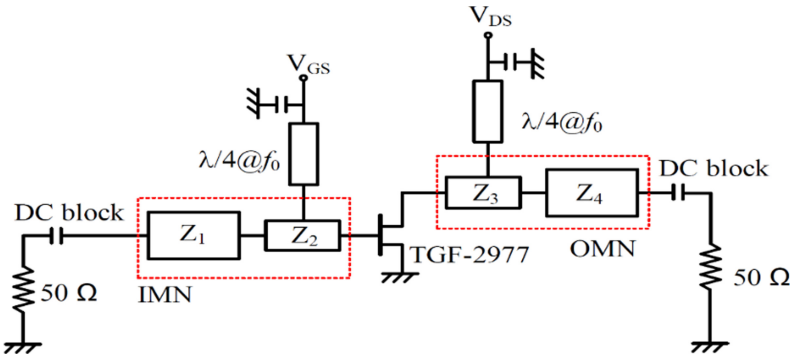

Fig. 3. Schematic of the proposed PA.

The input matching network (IMN) and output matching network (OMN) are implemented using two transmission lines with different characteristic impedances. These transmission lines function as low-pass filters [12]. It is noted that the IMN and OMN are designed at the fundamental frequency without using any harmonic termination elements. Here, Z1 = Z4 = 20 Ω; Z2 = Z3 = 150 Ω. The low pass filter technique [13] is employed to increase the PA bandwidth.

The optimum source and load impedance at the fundamental frequency (9.4 GHz) are: 25 – j92.8 Ω and 9.4 – j5 Ohm, respectively. These values were returned by using the Load Pull simulation in ADS software in which a GaN HEMT TGF2977-SM small-signal and large-signal models are provided by Qorvo [14]. Besides, the large-signal model of the GaN HEMT is constructed relying on a non-linear Angelov model. Figure 4 exhibits the EM model of the proposed schematic (see Fig. 3). The IMN and OMN are realized as microstrip lines with a RO4350B substrate in this figure.

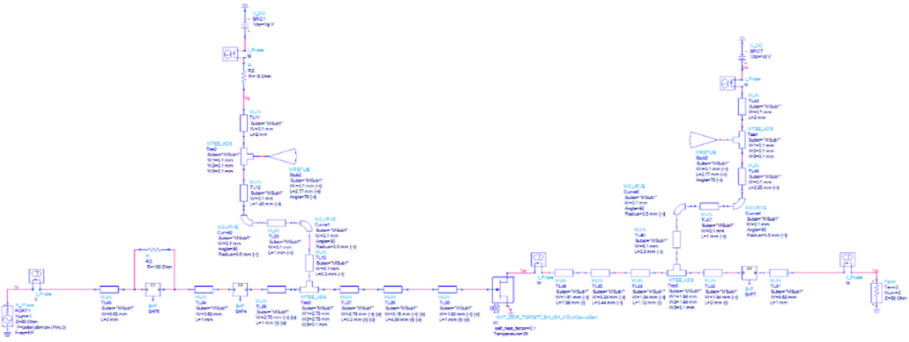

Fig. 4. Schematic of the proposed PA in ADS software.

The layout design of the proposed PA is shown in Fig. 5. The total PA dimension is 27.4 × 11.4 mm^2.

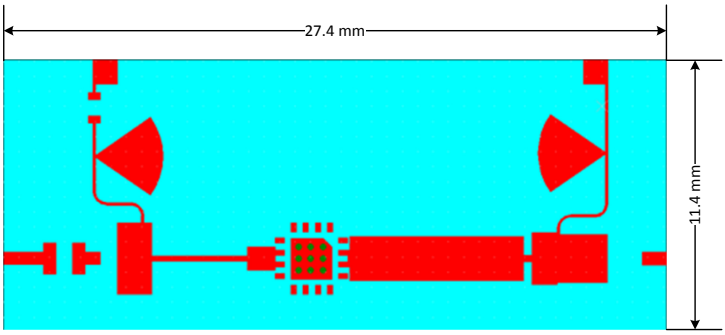

Fig. 5. The layout of the PA

Figure 6 indicates the simulated small-signal performance of the designed PA including input/output return losses, small-signal gain and stability. It can be seen that, both

input and output return losses exhibit low from 9 GHz to 10 GHz. The PA is stable in the frequency range with relatively high power gain.

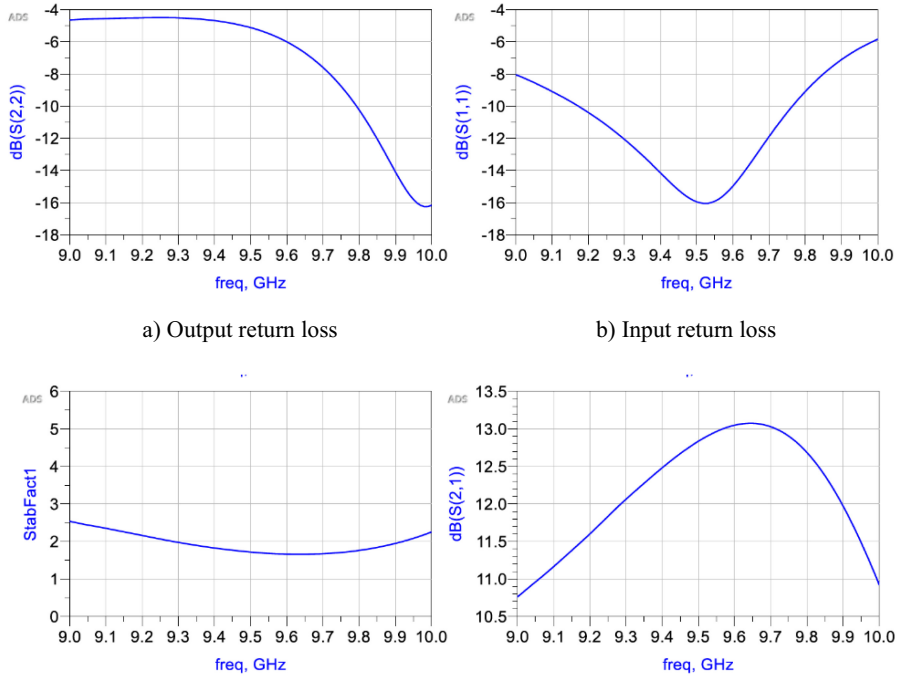

a) Output return loss

b) Input return loss

c) Stability factor

d) Small-signal gain

Fig. 6. Simulated small-signal performance.

The following Fig. 7 exhibits the simulated performance of the PA versus frequency for the large-signal model.

Obviously, the PA owns a relatively wide bandwidth in this characteristic. The variation of Pout is only below 2 dB in the frequency range of 9.0 GHz to 9.8 GHz and the PAE can be maintained at above 35%. Additionally, the saturated gain of PA is 12 dB with a 36-dBm output power at 9.4 GHz.

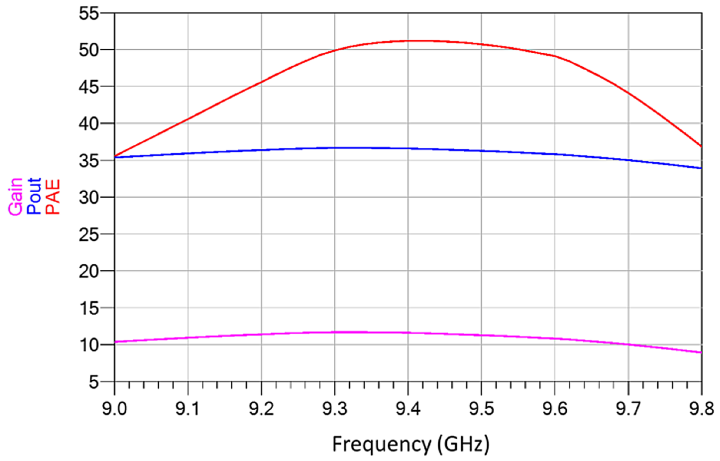

Fig. 7. Simulated large-signal performance

To maintain the high efficiency of PA for a wide range of output power, we utilize the supply modulation. The large-signal performance of the designed PA is evaluated and optimized by using a Harmonic Balance analysis in the ADS software. Figure 8 shows the large-signal performance of the designed PA for ten different fixed values of the drain bias voltage and modulated drain bias voltage at 9.4 GHz. When a drain bias voltage is properly controlled in range from 14 V to 32 V, the PA maintains a value of PAE higher than 40% in 10 dB of the output power back off.

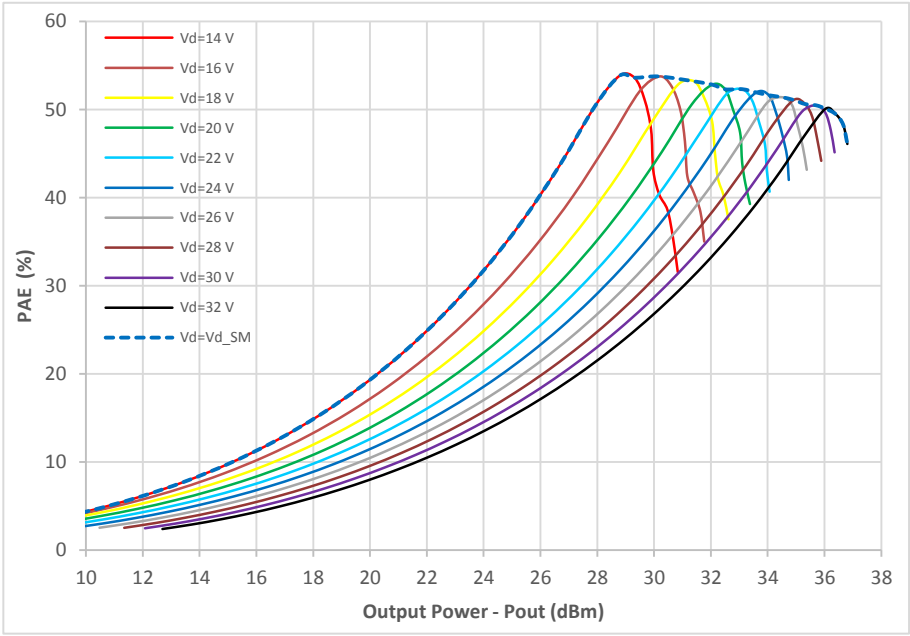

Fig. 8. PAE as a function of output power for 10 discrete supply voltages from 14 V to 32 V.

At the maximum output power trace, the PAE peak is about 50.1%, and it drops to 26.75% at 6 dB of the output power back off and 17.2% at 10 dB of the output power back off. However, the PAE of PA can reach 53.25% at 6 dB of the output power back off and 40.65% at 10 dB of the output power back off if using the supply modulation. This demonstrates that the PAE of PA is improved in a wide range of output power back off.

The PA is designed and optimized by using a priority criterion of high efficiency with low drain bias voltage and output power. This can improve the system performance even the AESA system works at its maximum distance because there are only a few of PAs (in the center of the array/sub-array) operates at the maximum output power and other PAs operates at the low output power.

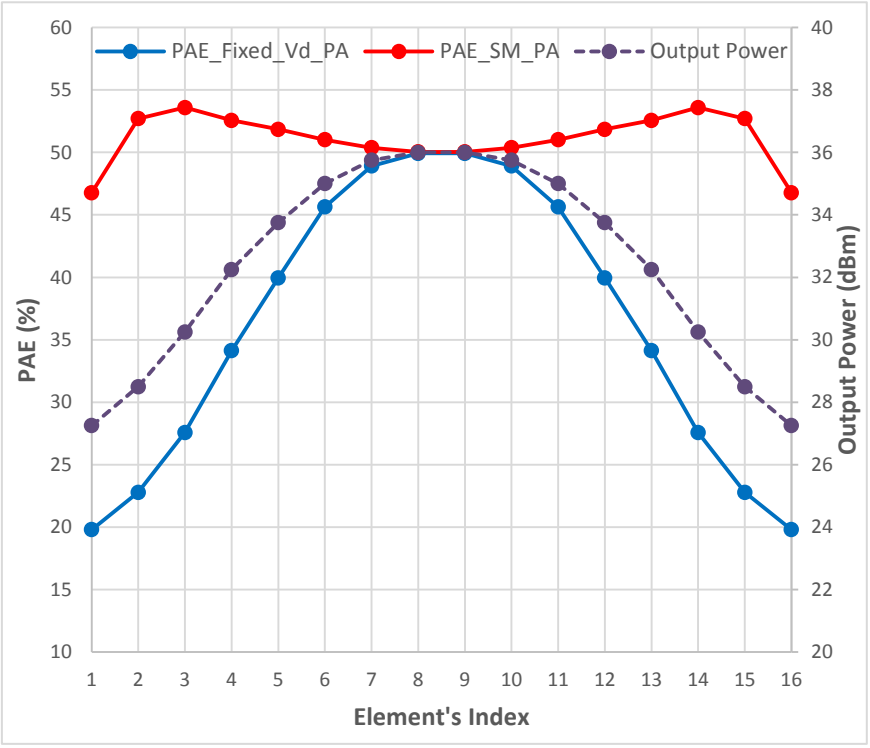

Fig. 9. PAE of a linear 16-element array using Taylor $\overline{n}$ distribution with n = 3 and −25 dB side lobe level (Color figure online)

Figure 9 shows the variation of PAE according to the position on a linear 16-element array using Taylor $\overline{n}$ distribution with $n = 3$ and a side-lobe level of −25 dB. We can see that the output power of array element declines from the center to edge of array (the dash line). This leads to reduction of the PAE of PAs using a fixed drain bias voltage Vd (the blue line). In contrast, the PAE of PAs can be significantly improved by using SM PAs (the red line).

4 Analysis Improvement Power Efficiency of AESA System with Designed GaN SM PA

In this section, we analyze the power efficiency of the AESA system using the proposed power amplifier (see Sect. 3) with various power distributions at different array scales and transmitting power levels. Here, we consider an AESA system working at the frequency of 9.4 GHz and using planar rectangular uniform arrays. The used power distributions for the side-lobe levels of −20, −25 and −30 dB are Chebyshev distributions denoted as Cheb_20, Cheb_25 and Cheb_30 respectively, and Taylor $\overline{n}$ distributions with $n = 2$, 3 and 4 abbreviated to TayN2_20, TayN3_25 and TayN4_30, respectively. Such power distributions are applied to both dimensions of the arrays.

Figure 10 shows the PAE variation of the AESA system with different array sizes: 4 × 16, 8 × 16 and 16 × 16 (rows x columns), where the dash lines indicate the systematic PAE when the PAs are supplied with fixed drain bias voltage for the maximum output power, the solid lines indicate the systematic PAE if using the SM PAs. Obviously, the solution using GaN SM PAs returns a significantly improved PAE (always higher than 48%) compared with the one using a fixed supply voltage (always lower than 37%).

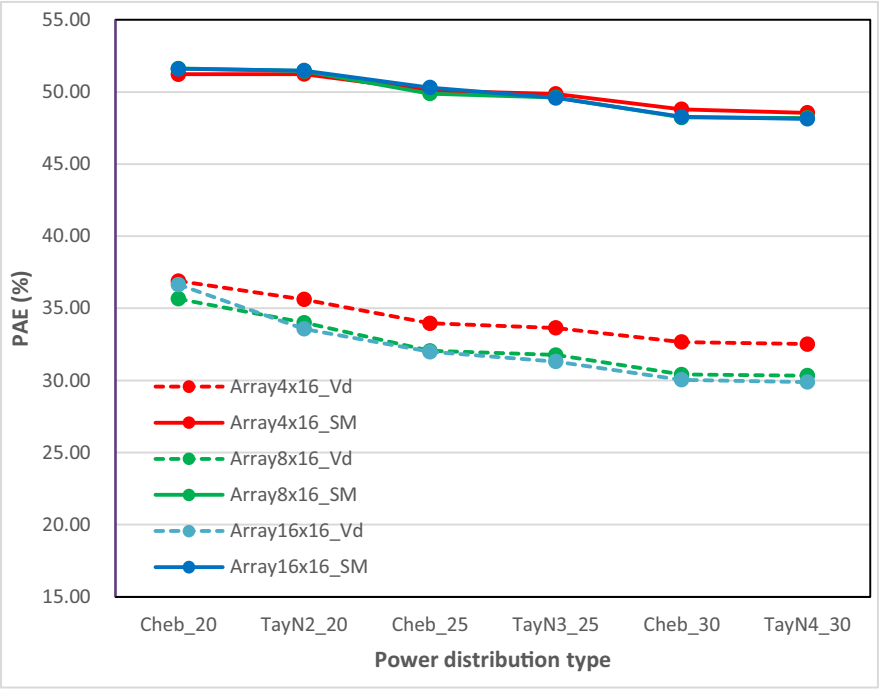

Fig. 10. PAE of AESA system with difference array scales and power distributions

Additionally, the lower side-lobe level, the lower PAE. The reason for that is that a lower side-lobe level needs a wider range of power distribution over the array aperture.

It means that there are many PAs working with the deeply low output power levels, corresponding to a low PAE.

The systematic PAE improvement is determined by the difference between the systematic PAEs using SM PA and using conventional PA, at the same other conditions (array size, output power etc.).

$$PAE_{Imp}(\%) = PAE_{SMPA}(\%) - PAE_{Conv}(\%) \tag{9}$$

where, PAE_{Imp} is the systematic PAE improvement, PAE_{SMPA} is the systematic PAE using the SM PA, and PAE_{Conv} is the systematic PAE using the conventional PA.

With the same output power condition, the systematic PAE improvement with the distribution types and array sizes is revealed in Table 1.

Table 1. The systematic PAE improvement (%) of AESA system by using GaN SM PAs.

Array size	Chebyshev distribution			Taylor $\bar{n}$ distribution		
	−20 dB	−25 dB	−30 dB	−20 dB (n = 2)	−25 dB (n = 3)	−30 dB (n = 4)
4 × 16 element	14.33	16.14	16.13	15.62	16.22	16.03
8 × 16 element	15.97	17.83	17.82	17.44	17.85	17.87
16 × 16 element	14.95	18.31	18.23	17.91	18.28	18.24

As shown in Table 1, the systematic PAE is improved from 14.33% to 18.28%. In most cases that systems with larger array (16 × 16 element) have efficiency better than others with smaller arrays (4 × 16 and 8 × 16 element) with the same power distribution.

In next step, we consider the systematic PAE improvement by using SM PA according to the variation of transmitting power.

Figure 11 shows the systematic PAE of an AESA system with 16 × 16-element array when the output power decreases 0 dB to 6 dB from maximum output power. It can be seen that its PAE also decreases when the output power decreases. However, the solution using GaN SM PAs outperforms the one using fixed drain bias voltage PAs because the power efficiency grows according to the reduced level of output power. This is shown in Fig. 12.

In short, the analysis results show that the use of GaN SM PAs significantly improves the power efficiency of an AESA system with using power distribution for synthesizing a beam pattern, reducing side-lobe level and transmitting power variation. The improved power efficiency is really meaningful for systems with a large number of elements and to reduce transmitting power.

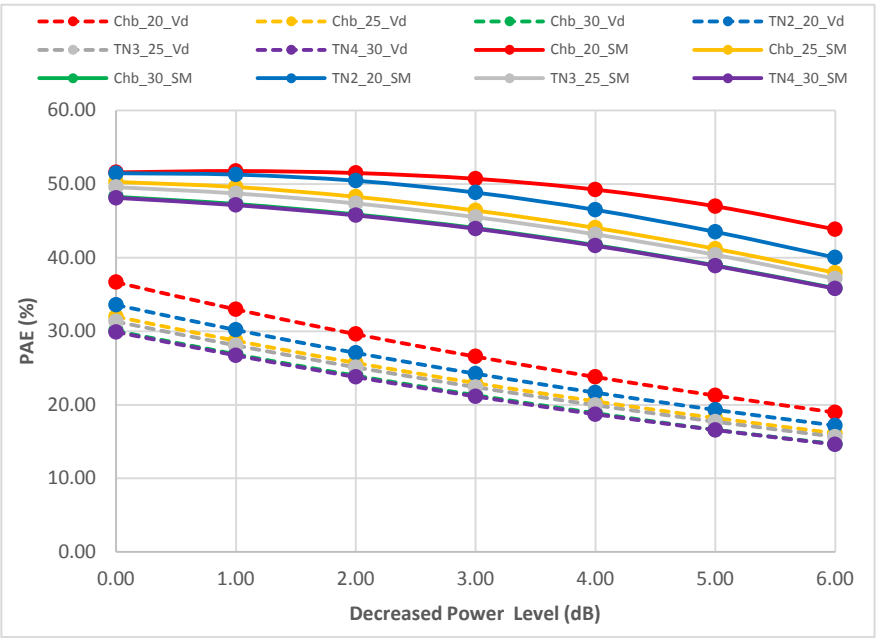

Fig. 11. PAE of AESA system vs decreased power level

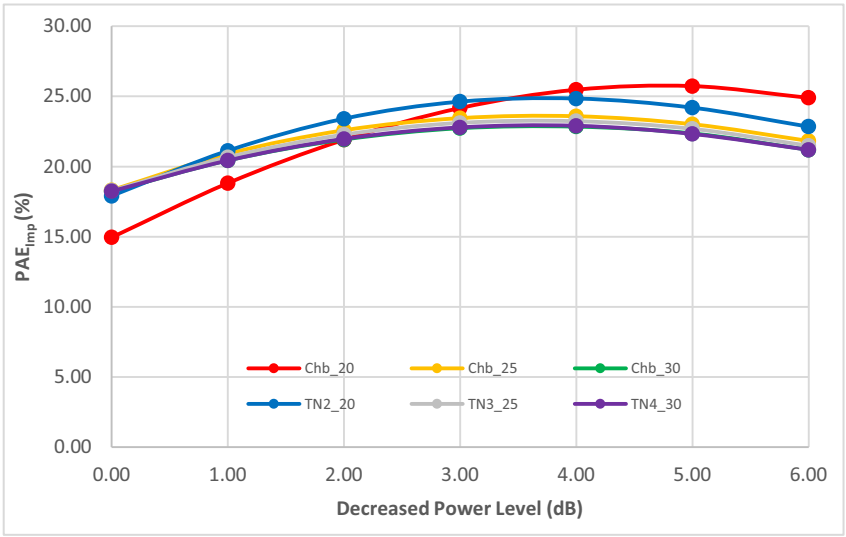

Fig. 12. The systematic PAE improvement versus decreased power level

5 Conclusion

The paper investigates the inequivalent power distribution on the antenna aperture of an AESA system resulting from synthesizing a beam pattern in order to reduce the side-lobe level and allow to alter its power corresponding to operating ranges. The working mode in which the established power is lower than its designed maximum level cannot achieve the highest efficiency. Therefore, the system can be heated up due to emitting useless energy during its operation. These challenges cooling the system, thus degrading it. Accordingly, the paper proposes using GaN SM PAs to improve the power efficiency. These PAs are high-efficiency elements and they can maintain a high efficiency in a wide range of output back off power. Moreover, a GaN PA needs a high drain bias voltage to function properly, thus allowing to control the PA conveniently in a wide range. The paper also introduces a 4-W X-band GaN SM PA designed for an AESA system. The low-pass filtering technique used in the proposed design provides the impedance-matching ability and expands the bandwidth. Thus, the PA can obtain a PEA of above 35% in a frequency range of 9.0 GHz to 9.8 GHz, and higher 40% in 10 dB of the output power back off at 9.4 GHz. The simulation results show that the proposed method significantly improves the power performance compared with current approaches using other amplifiers.

References

1. Hommel, H., Feldle, H.-P.: Current status of airborne active phased array (AESA) radar systems and future trends. In: Proceedings of IEEE MTT-S International Microwave Symposium Digest, Long Beach, CA, pp. 1449–1452 (2005)
2. Feldle, H.: State of the active phased array technology. In: Proceedings of 2007 2nd International ITG Conference on Antennas, Munich, pp. 241–245 (2007)
3. van Bezouwen, H., Feldle, H., Holpp, W.: Status and trends in AESA-based radar. In: Proceedings of IEEE MTT-S International Microwave Symposium, Anaheim, CA, pp. 526–529 (2010)
4. Mishra, A.K.: AESA radar and its application. In: Proceedings of 2018 International Conference on Communication, and Computing, Chennai, India, pp. 205–209 (2018)
5. Hansen, R.C.: Phased Array Antennas, 2nd edn. Wiley, Hoboken (2009)
6. Popovic, Z.: GaN power amplifiers with supply modulation. In: Proceedings of 2015 IEEE MTT-S International Microwave Symposium, Phoenix, AZ, pp. 1–4 (2015)
7. Cappello, T., Florian, C., Niessen, D., Paganelli, R.P., Schafer, S., Popovic, Z.: Efficient X-band transmitter with integrated GaN power amplifier and supply modulator. IEEE Trans. Microw. Theory Tech. **67**(4), 1601–1614 (2019)
8. Yan, H., Ramesh, S., Gallagher, T., Ling, C., Cabric, D.: Performance, power, and area design trade-offs in millimeter-wave transmitter beamforming architectures. IEEE Circuits Syst. Mag. **19**, 33–58 (2019)
9. Mailloux, R.J.: Phased Array Antenna Handbook, 2nd edn. Artech House Inc., Norwood (2005)
10. Skolnik, M.I.: Radar Handbook, 3rd edn. McGraw-Hill, New York (2008)
11. Winslow, T., et al.: Advances in GaN technology and design for active arrays. In: Proceedings of 2013 IEEE International Symposium on Phased Array Systems and Technology, Waltham, MA, pp. 1–19 (2013)
12. Hong, J.-S.: Microstrip Filters for RF/Microwave Applications, 2nd edn. Wiley, Hoboken (2011)

13. Rabbi, K., et al.: Highly efficient wideband harmonic-tuned power amplifier using low-pass matching network. In: Proceedings of 2017 47th European Microwave Conference (EuMC), Nuremberg, pp. 292–295 (2017)
14. https://www.qorvo.com/